CRYOBIOLOGY **34,** 394–405 (1997)
ARTICLE NO. CY972010

Gross Damage Accumulation in Frozen Rabbit Liver Due to Mechanical Stress at Cryogenic Temperatures

Yoed Rabin,*,† Peter Olson,‡ Michael J. Taylor,§ Paul S. Steif,*
Thomas B. Julian,† and Norman Wolmark†

**Department of Mechanical Engineering, Carnegie Mellon University, 5000 Forbes Avenue, Pittsburgh, Pennsylvania 15213-3890; and ‡Department of Laboratory Medicine, §Cryobiology Research Program, and †Department of Human Oncology, Allegheny University of the Health Sciences, 320 East North Avenue, Pittsburgh, Pennsylvania 15212-4772, U.S.A.*

The second phase of a pilot study dealing with the mechanical response of frozen biological tissues to external compressive load is presented. This stage deals with histological observations of the damage accompanying mechanically induced permanent deformation in frozen rabbit liver. No significant gross histological damage was observed in the liver samples due to either processing the tissue in the frozen state, due to slow cooling of the liver tissues down to −20°C, or due to rapid cooling of the samples down to −196°C. No histological changes were observed in tissue samples that were loaded within the elastic regime, that is, below the yield strength of the material. Therefore, it is concluded that histological changes due to mechanical stresses are associated with plastic (permanent) deformations. Histological observations indicate that linear cracks which appear to have no preferred orientation develop due to mechanical stress beyond the yield strength of the frozen tissue. These cracks accumulate until final failure of the frozen tissue, when the tissue sample collapses to rubble. Based on histological observations and concepts from solid mechanics, an interaction between crack formation and irregularities in the frozen medium is suggested. Significant sources for such irregularities, in an homogeneous tissue such as the liver, are blood vessels and bile ducts. These irregularities may either initiate crack formation or, on the other hand, may also arrest propagating cracks.

The mechanisms of cryodestruction may generally be separated into two groups, depending on the degree of phase transition. The first group includes destruction mechanisms within the phase transition temperature range and is related to the dynamics of the freezing/thawing processes. The temperature range of phase transition is dependent on the chemical content of the solutions of the cryotreated tissue and on its cooling history (6, 13). When cooling quasistatically, the phase transition range is typically between 0 and −22°C (assuming that body solutions behave like $NaCl-H_2O$). However, the lower boundary of phase transition decreases as the cooling rate increases due to the departure of the transport phenomena from near equilibrium conditions; it also decreases when nucleation sources are absent (9–12). The lower boundary of phase transition can easily reach −45°C in biological systems (2). Mechanical interaction between ice crystals and cells also enhances the destruction during the phase transition process, causing localized mechanical stresses on cells (8).

The second group of destruction mechanisms is related to destruction occurring after phase transition has completed, i.e., in the solid state, and therefore is related to mechanical stress. For example, stresses can arise due to the dramatic volume changes that take place during the liquid–solid phase change process (1). Stresses can also develop when temperature gradients within the frozen tissue produce nonuniform thermal contraction. These temperature gradients are present when the tissue is brought to the cryogenic temperature range during typical cryosurgical or cryopreserva-

Received October 21, 1996; accepted February 12, 1997.

0011-2240/97 $25.00

tive cooling protocols (3, 5, 7, 15). These mechanical stresses act as a destruction mechanism by causing permanent deformations (beyond the elastic limit) and/or cracking in the frozen tissue. Typically, cracking occurs instantaneously when the stresses in some region reach some critical level. Damage may also develop due to static fatigue (17), in which subcritical crack growth occurs very slowly at persistent stresses that are lower than those required for instantaneous fracture. Such cracks may eventually grow to such a size that instantaneous fracture can occur. Slow crack growth tends to decrease with decreasing temperature and to increase with increasing stress. One expects that static fatigue plays a significant role only when tissues are stored at cryogenic temperatures for long periods of time.

It has been suggested that elastic deformations resulting from mechanical stresses due to constrained contraction of the frozen tissue (also termed thermal stresses) may cause mechanical damage to cell membranes (18). It was demonstrated theoretically that, for a spherical cryoprobe and typical physical properties of ice, the thermal stress can easily reach the yield strength of the frozen tissue (15). It was therefore proposed that thermal stresses which produce plastic (permanent) deformation of the frozen tissue may severely increase the mechanical damage to the cell's membrane and to the tissue structure. The analysis accounted for plastic deformations by assuming an elastic perfectly-plastic model for the mechanical response of the freezing tissue. The analysis in (15, 18) revealed that both tensile and compressive stresses exist in any cryoprocedure. However, it is expected that the compressive strength of brittle materials such as frozen biological tissues is higher than the tensile strength (16).

To gain some insight into the mechanical properties of frozen soft biological tissues, the response of frozen rabbit liver, kidney, and brain to externally applied compressive stresses was investigated (16). The main concept underlying this study was that the stresses associated with the constrained contraction of the frozen tissue, i.e., due to temperature variations within the frozen tissue, can be simulated by an external mechanical load which is applied to the frozen tissue while it is maintained at a uniform temperature. The rationale for this concept is well established in the study of deformable bodies: the deformations associated with stress are not dependent on the origin of the stress. The response of the frozen tissue to an external load is a function of many factors such as the percentage of blood and other body fluids per unit volume of tissue, chemical content, properties of the extracellular matrix, fiber strength, and orientation.

A unique response of frozen soft biological tissues to compression is reported by Rabin *et al.* (16). The frozen tissue was found to have an elastic behavior up to rather small strains, on the order of 0.005, and a sawtooth pattern of stress thereafter, featuring a series of sudden stress drops followed by a linear return to a roughly constant upper level of stress. It was suggested that the stress drops may be associated with the formation of cracks which steadily accumulate until final failure. The highly heterogeneous nature of this material may allow such cracks to appear, but not to propagate. Complete unloading leaves the material with a permanent plastic strain; continued cracking only resumes when the stress is returned to the previous level at which cracking occurred. The jagged nature of the curves notwithstanding, it appears that the mechanical response of frozen tissues can usefully be idealized by an elastic perfectly plastic model.

The present paper, dealing with histological observations of frozen rabbit liver subject to various levels of compressive stress, is the second phase of the study presented by Rabin *et al.* (16).

MATERIALS AND METHODS

The experimental apparatus is based on a standard mechanical testing system. The load is applied by an hydraulic piston, with accurate control of the rate of loading. The load magnitude is measured by a load cell which is an integral part of the standard load device.

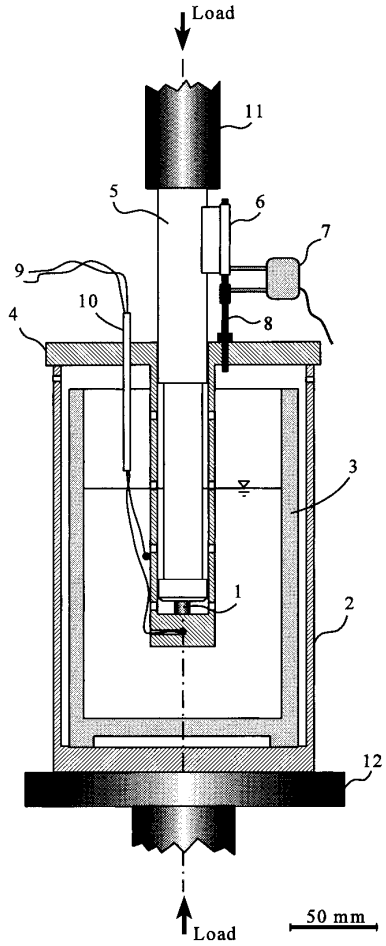

FIG. 1. Schematic presentation of the load chamber of the experimental apparatus for compression tests of frozen tissues at cryogenic temperatures (16).

As illustrated in Fig. 1, a special loading chamber has been designed and constructed to accommodate the frozen tissue sample during the tests. In order to maintain a constant cryogenic temperature, the tissue sample was immersed in liquid nitrogen while the experiment was performed.

With reference to Fig. 1, the load carrying components of the chamber are: shell **2,** which rests on ram **12;** cover **4,** which rests on the shell, consisting of an annular disk to which is welded a capped tube; and column **5,** which presses against the stationary platen **11** on its upper end and bears on the tissue sample **1** on its lower end. Hence, if the steel components are viewed as essentially rigid, then the upper face of the tissue sample **1** is held stationary, while its lower face displaces upward with the tube cap, tube, disk, and shell which are rigidly driven by the ram **12.** The displacement of cover **4** relative to column **5** is measured by extensometer **7.** One arm of the extensometer is connected to column **5** by fixture **6,** while the other arm is connected to disk **4** by rod **8.** A hole in fixture **6** acts a guide for the upper end of rod **8.** The experimental setup is described in more detail in (16).

Temperatures were monitored at two points by copper–constantan thermocouples, **9.** One thermocouple was located at the center of the cap of cover **4,** while the other was attached to the tube, above the tissue's upper surface. The second thermocouple served as a liquid nitrogen level indicator; it shows the liquid nitrogen boiling temperature as long as the sensor is below the coolant level.

Tissues to be used in the compression tests were obtained from four New Zealand White rabbits (2.5–4 kg) by excising the liver soon after death. These organs were procured from rabbits that had been sacrificed for other studies in which the heart was excised under general anesthesia of halothane (2.5 liters/min) admin-

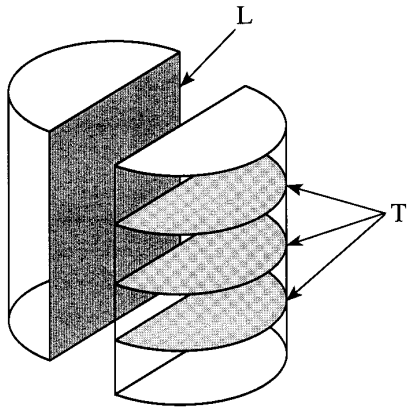

FIG. 2. Schematic presentation of the longitudinal (L) and transverse (T) cross-sections that were taken for histological observations.

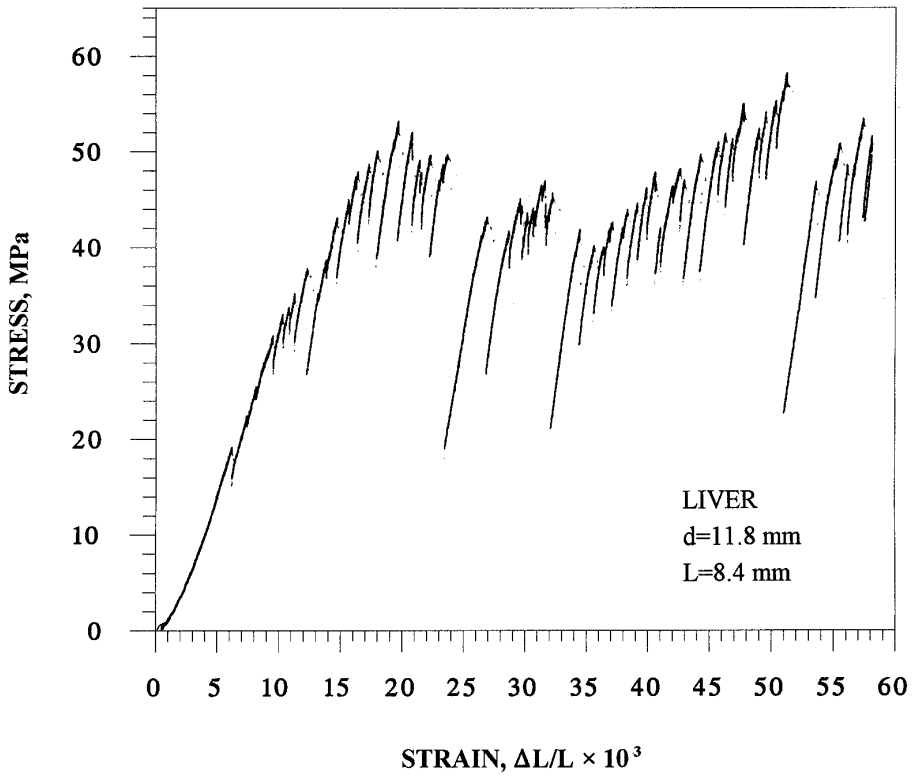

FIG. 3. Typical stress-strain relationship obtained from a load test of a rabbit liver sample.

istered via a ventilator. These procedures were carried out in accordance with the guidelines and standards of the United States Public Health Services for use and care of laboratory animals and with the approval of the Institutional Animal Care and Use Committee of the Allegheny-Singer Research Institute.

Compression tests were performed on frozen cylindrical tissue samples prepared as follows: The fresh organ, i.e., liver, was excised from the body and placed on a flat plastic tissue culture dish. The dish was sealed and placed immediately in a freezer, maintained at −20°C, for a period of 72 h. The sealing was required in order to avoid drying of the tissue surface. Special care was taken to avoid blood losses from the liver. Using a cylindrical cutting tool (16), cylindrical samples were cut out from the frozen liver. Cutting and shaping the tissue sample was accomplished in a few minutes, without any significant thawing of the frozen liver. The shaped cylindrical sample was then immersed immediately in liquid nitrogen and kept at −196°C until the compression test was performed, a day or two later. Cutting tools having an inner diameter of 8.7 and 11.8 mm were used. The ratio of the height to the diameter of each sample was kept in the range of 0.8 to 1.5.

Prior to experimentation, shell **2** (Fig. 1) was placed on the load device, and container **3** was placed inside the shell and filled with liquid nitrogen. The tube of cover **4** and column **5** were precooled for a few minutes. The tissue sample was transferred in the frozen state and placed on the upper surface of the cap of the tube. The column was inserted into the tube so that rod **8** slides into fixture **6.** Cover **4** was placed on shell **2,** while the tissue sample, together with a part of the column and a part of

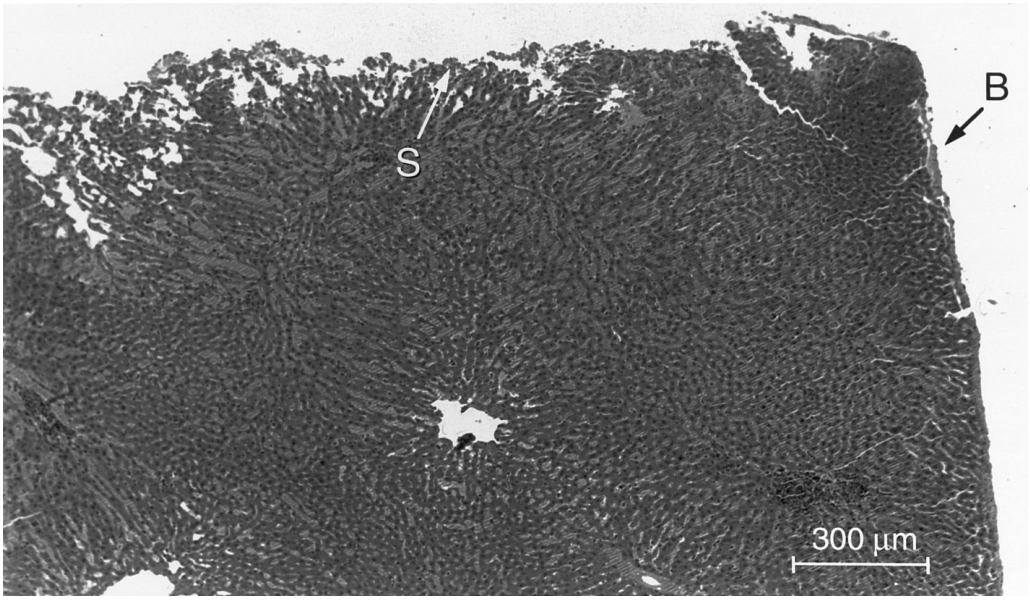

FIG. 4. A longitudinal cross-section of a control tissue sample which was frozen to −20°C, shaped as a cylinder, and thawed with no loading. Damage caused to the outer surface of the frozen cylindrical sample (S) due to the cutting in the frozen state is minimal. This damaged tissue layer was found to have an average thickness of 0.1 to 0.2 mm. No cracks associated with mechanical stresses were observed in the control sample. The ragged surface was produced by shearing of the frozen tissue, resulting in artifactual changes consisting of stretching and fragmentation of cells, as well as minute chunks of tissue that have been torn away. The artifacts are seen only on the cut surface; the base (B) ends do not show these changes.

the tube, were immersed in the liquid nitrogen. Finally, the extensometer arms were connected by rubber bands to fixture **6** and rod **8.**

The experiment was started after all parts reached thermal equilibrium. The thermal equilibrium was observed as the extensometer signals decay; i.e., no relative movement was observed between the cover and the beam. Finally, the test was performed under displacement control, with a velocity of 1.4×10^{-3} mm/s, which yielded an average strain rate of 10^{-4} s^{-1}. The values of load as a function of the relative displacement at the extensometer were plotted and the thermocouples temperature were monitored. The precooling period took about 15 min for the first test and from 2 to 3 min for each of two successive tests. Each compression test took from 3 to 10 min.

Tissue samples were taken for histological observation at six different points along the freezing-loading procedures as follows: (1) fresh liver samples as a control; (2) samples that were frozen to −20°C and shaped as a frozen cylinder; (3) cylindrical samples that were further cooled to −196°C without loading; (4) cylindrical samples that were loaded in the elastic regime, at −196°C; (5) cylindrical samples that were loaded up to the plastic regime, after several stress drops had taken place; and (6) samples that were loaded up to a complete failure; i.e., the cylindrical sample collapsed to rubble. The tissue samples were thawed at the room temperature by natural convection of air. After complete thawing the tissue samples were immersed in 10% buffered formalin solution for 48 h.

Histological preparations were made from four samples at each of the six points described above. With reference to Fig. 2, the cylindrical tissue samples were first cut along the center line of the cylinder to produce a

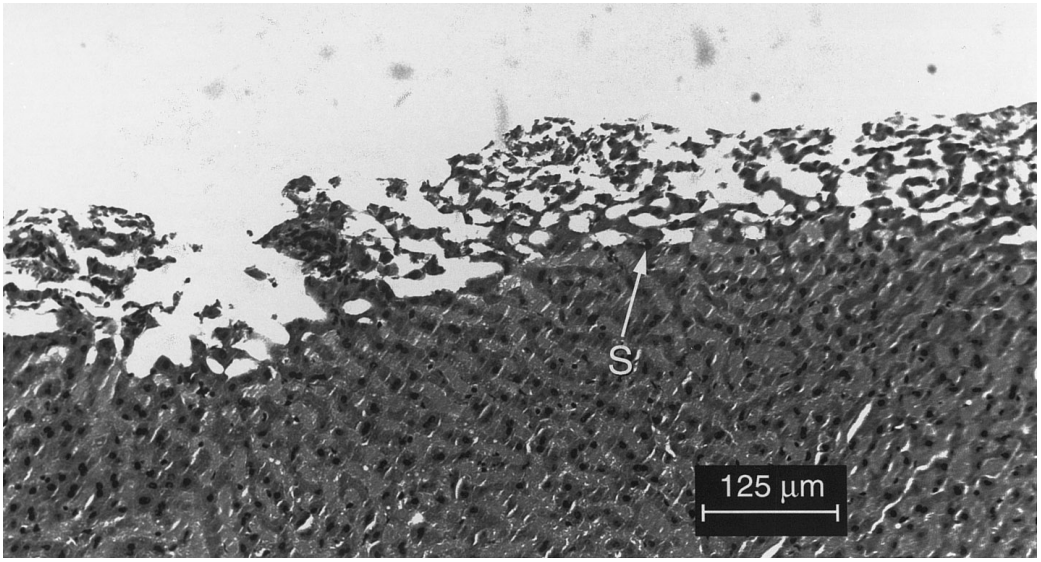

FIG. 5. A longitudinal cross-section of a control tissue sample which was frozen to −20°C, shaped as a cylinder, cooled down to −196°C, and thawed with no loading. No additional damage beyond that appearing in Fig. 4 is observed on the outer surface of the cylindrical sample (S), which suggest that no thermal stress beyond the yield strength has developed in the tissue during the cooling protocol.

longitudinal cross-section (L). One-half of the cylinder was then cut in a few locations, parallel to the bases, to produce transverse cross-sections (T). One block of the tissue from the longitudinal plan and another block containing three different transverse levels were processed by routine surgical pathology techniques. The formalin-fixed tissue was placed in an automatic tissue processing machine to dehydrate the tissue and replace cellular water with paraffin. The wax-embedded tissue was cut into sections 5 μm thick with a microtome and then mounted on glass slides. The tissue was stained using hematoxylin and eosin stains which differentiate cell nuclei from cytoplasm for viewing by light microscopy.

RESULTS AND DISCUSSION

A representative stress–strain curve for liver tissue under compression is presented in Fig. 3. The ram moves steadily (and hence the strain increases steadily) from the beginning to the end of the test. Following a roughly linear regime, the stress suddenly drops. Since displacement is controlled, the stress drop represents a sudden drop in the material's load carrying capacity. The stress then increases to a somewhat higher level at which point an additional stress drop occurs. After some number of stress drops (each generally at an increasingly higher level of stress), an upper level of stress is reached.

To summarize the observations, we have found elastic (that is, essentially reversible) behavior up to rather small strains, on the order of 0.005, and a sawtooth pattern of stress thereafter featuring a series of sudden stress drops followed by a linear return to a roughly constant upper level of stress. The stress drops are on the order of one-third to one-half of the upper level of stress. The linear returns to the upper stress level occur with a slope that is close to the initial slope. At any point the stress can be reduced to zero, leaving a permanent strain; reloading causes the unloading $\sigma-\epsilon$ curve to be retraced back up to the upper level of stress at which point the stress drop phenomenon reappears. Final failure, which

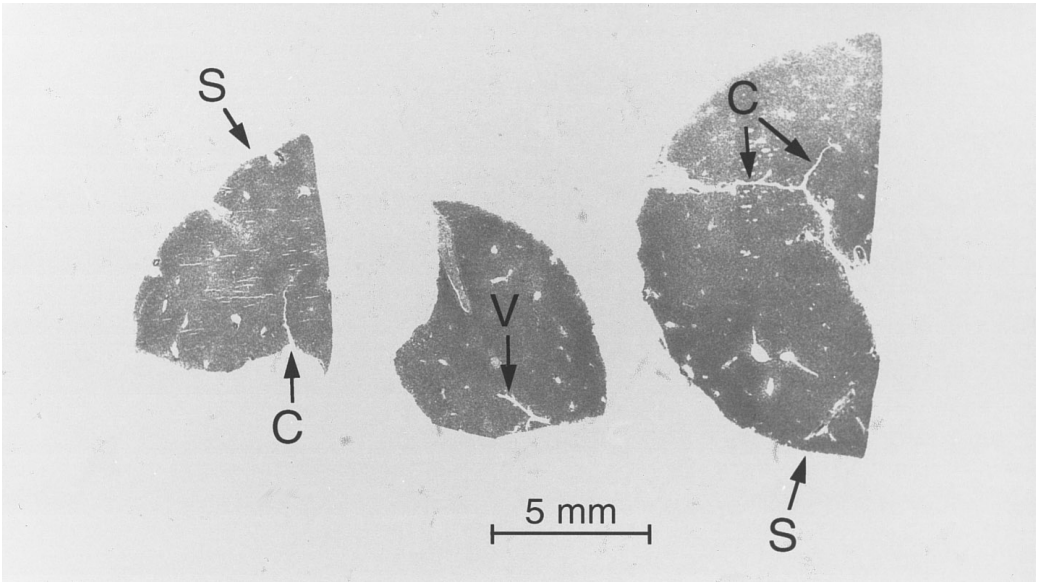

FIG. 6. Low-power magnification of transverse cross-sections of a tissue sample which was loaded beyond its yield strength. The tissue sample was unloaded prior to a complete failure, i.e., the tissue sample kept its cylindrical shape after unloading in the frozen state. The cracks (C) appear to have no preferred orientation. Some of the cracks are easily observed in low-power magnification views as presented here and in Fig. 7, while others demand higher magnification (Figs. 8–10). S, the outer surface cylindrical sample; V, a blood vessel. The cracks and the blood vessels can be more readily distinguished at higher magnifications, such as in Fig. 10.

generally reduces the specimen to rubble, occurs at strains on the order of 10 times that at which the first stress drop appears.

It is well known that the mechanical response of solid materials can be strain-rate dependent. Experimental data with regard to the dependence of water ice on strain rate are available for relatively high temperatures, close to the freezing temperature. For pure water ice, both the strength and the yield strain increase with strain rate, and decrease with temperature (4). For sea water ice, the dependence on the strain rate is more complicated and is related to the solution concentration as well (19); note that sea water ice may better resemble frozen biological tissues. However, the strain rate effect at −196°C, when the frozen tissue is expected to behave like a brittle material (14), is likely to be rather weak. The strain–rate of 10^{-4} s^{-1}, which was used in this study, is very standard for mechanical testing of solid materials at low strain rates.

We now turn to the histological observations. Figures 4 and 5 present control samples which were frozen and shaped into a cylindrical shape in the frozen state, but were not loaded (points 2 and 3 along the freezing–loading procedures described above, respectively). From Figs. 4 and 5 it can be seen that no significant damage was caused to the gross structure of the liver tissue due to either cooling to −20 or −196°C. It can further be seen that the damage caused to the outer surface of the frozen cylindrical sample (S) due to the cutting in the frozen state is minimal. This damaged tissue layer was found to have an average thickness of 0.1 to 0.2 mm. No cracks associated with mechanical stresses were observed in the control sample. The control tissue frozen to −20°C has a ragged surface produced by shearing of the frozen tissue resulting in artifactual changes consisting of stretching and fragmentation of cells, as well as minute chunks of tissue that have been torn

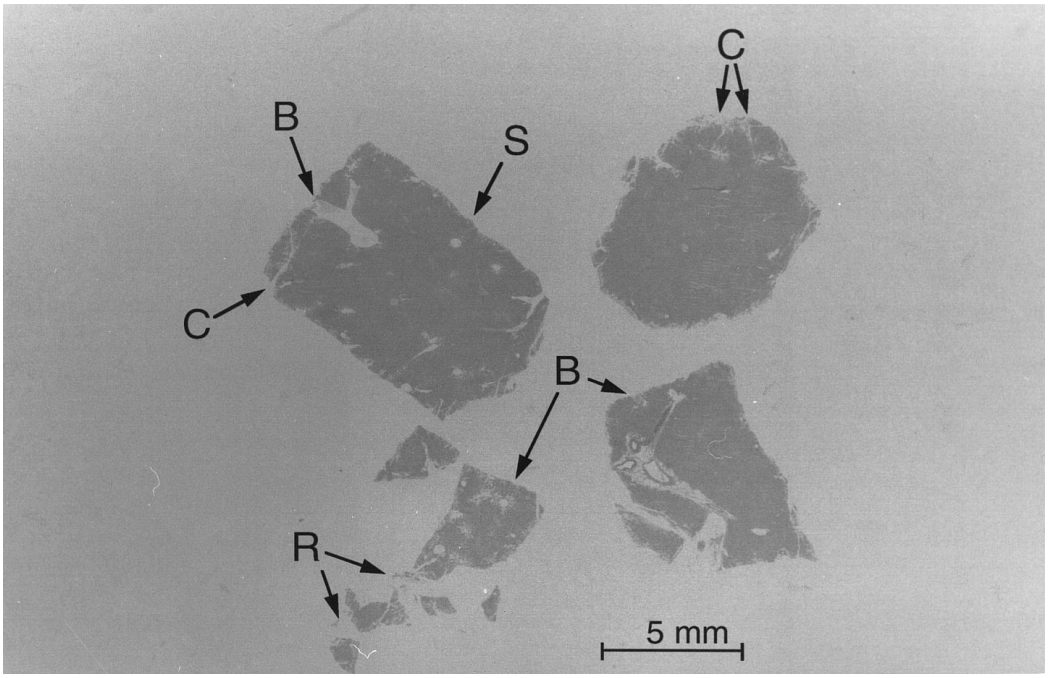

FIG. 7. Low-power magnification of a longitudinal cross-section of a tissue sample which was loaded beyond its yield strength. B, the bases of the cylindrical sample; C, cracks; R, a part of the tissue sample which turned into rubble; S, the outer surface of the cylindrical sample.

away. The artifacts are seen only on the cut surface; the base (B) ends do not show these changes.

No histological changes were observed in tissue samples that were loaded within the elastic regime, that is below the yield strength: the stress at which the first stress drops appear. Therefore, discussion of tissue damage focuses on the plastic regime, that is points 5 and 6 along the freezing–loading procedure described above. Figures 6 and 7 present cross-sections in the transverse and longitudinal directions, respectively, of samples that were loaded beyond the yield strength of the frozen tissue. As can be seen from both figures, the cracks (C) do indeed form and have no preferred orientation. Some of the cracks are easily observed in low power magnification views such as in Figs. 6 and 7, while others demand higher magnification. Both tissue samples presented in Figs. 6 and 7 were unloaded prior to a complete failure of the cylindrical sample; i.e., the tissue samples kept their cylindrical shape after unloading in the frozen state. However, some of the tissue samples changed into rubble after thawing as designated by R in Fig. 7.

Figures 8 and 9 show a longitudinal cross-section at high power magnification. The applied load acts in the direction of the arrow F in Fig. 8. Note that there is no obvious preferred crack orientation relative to the applied load. For comparison, during the compressive loading of more extensively studied brittle materials such as ice or rocks, cracking tends to initiate on planes that are oriented at roughly 45 degrees from the compression axis; the faces of cracks lying along such planes experience sliding relative to each other. The limited observations of cracking in frozen tissue presented here, with cracks neither parallel nor perpendicular to the loading direction, are not inconsistent with the cracking pattens in other brittle materials.

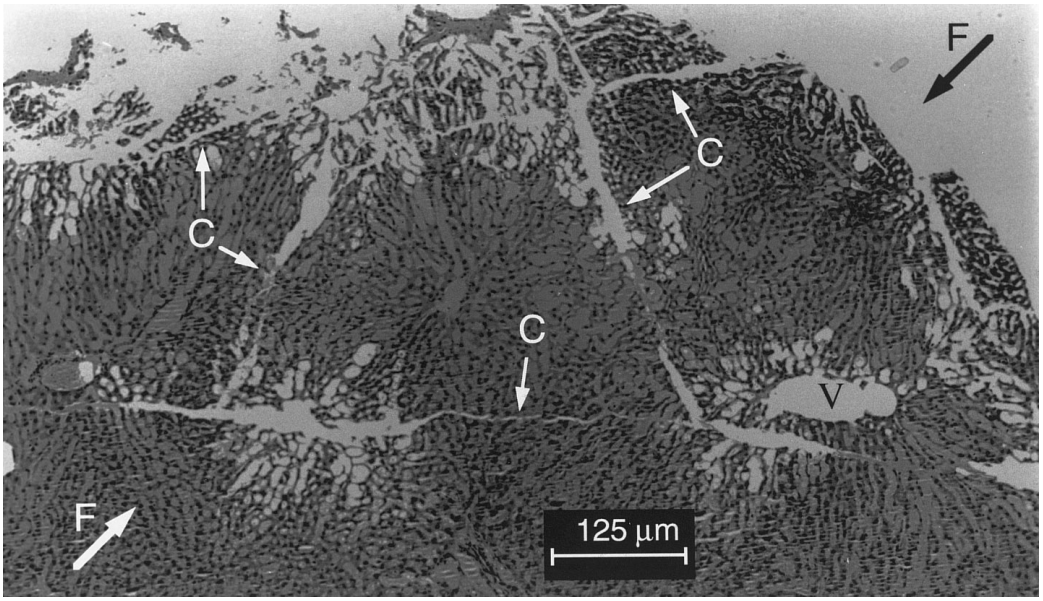

FIG. 8. High-power magnification of the top right portion of the tissue sample presented in Fig. 7. The applied load acted in the direction of the arrows F. V, a blood vessel.

In general, whether the loading is tensile or compressive, cracks or damage in materials tend to initiate in regions of inhomogeneity: in such regions, the stresses tend to be higher. An example of this can be seen in Fig. 10, depicting a crack which has formed in the vicinity of blood vessels, which represent a substantial irregularity in the frozen medium. Such irregularities can play a quite different role as well. Say a crack has formed already and is propagating. Generally, if the material is homogeneous ahead of the crack, then propagation will continue unabated. However, if the crack encounters a different material or an irregularity, then crack propagation can be halted or diverted. Thus, the same irregularities in the frozen medium which are the source of crack initiation, such as blood vessels and bile ducts in the liver, may also limit crack propagation. Indeed, the highly heterogeneous structure of tissues may be critical in permitting the substantial degree of cracking that occurs prior to final failure.

Close inspection of the cracks shows that they create sharp angles with respect to one another, which are not seen in frozen tissue that has not been stressed; by contrast, irregular tears may be seen due to handling of the tissue prior to embedding in wax. Note in Fig. 9 that cells along the crack have sharp edges without pieces being torn away. The large empty spaces between cells along the cracks indicate cell rupture and a loss of the cells' capability of retaining the intracellular content after the formation of the adjunct crack and the subsequent thawing. Other cells in these areas appear degenerated with darkening of both cytoplasm and nuclei. Cells lining the crack are fractured. The cracks often tend to connect large blood vessels as seen in Fig. 10.

SUMMARY AND CONCLUSIONS

The second phase of a pilot study dealing with the mechanical response of frozen biological tissues to external compressive load is presented. This stage deals with histological observations of the damage accompanying mechanically induced permanent deformations in frozen rabbit liver. The main concept behind this study is that the mechanical load

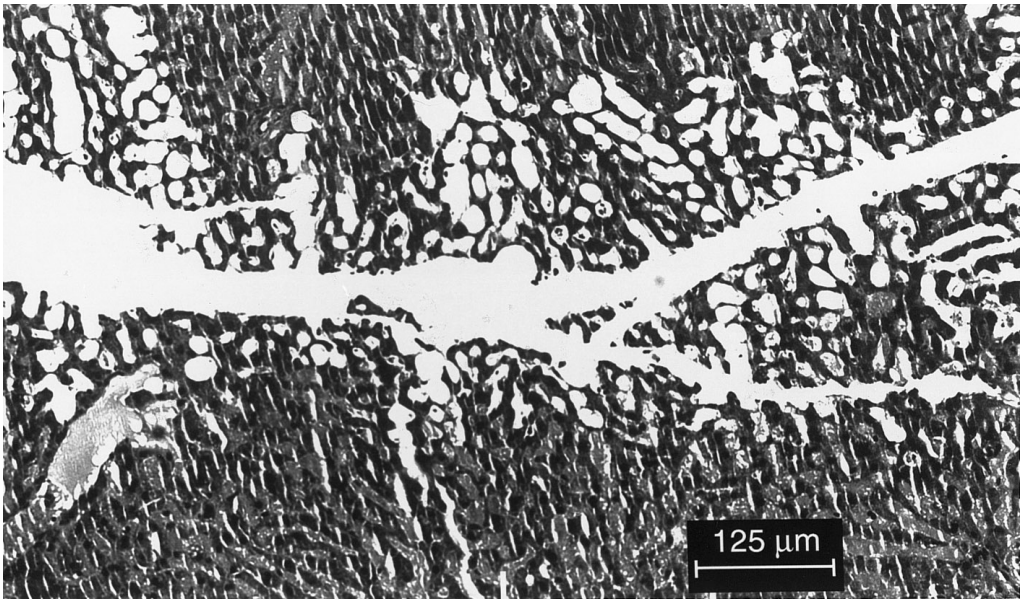

FIG. 9. High-power magnification of the top left portion of the tissue sample presented in Fig. 7. The large empty spaces between cells along the cracks indicate cell rupture and a loss of the cells' integrity and retention of the intracellular solution after the formation of the adjunct crack and the subsequent thawing. Cells lining the crack are fractured.

due to the constrained contraction of the frozen tissue, i.e., due to temperature variations within the frozen region, can be simulated by an external mechanical load which is applied directly to the frozen tissue, which is held at a uniform temperature. The rationale for this concept is well established in the study of deformable bodies: the deformations associated with stresses are not dependent on the origin of the stress.

The following freezing–loading protocol was applied in the present study: liver tissues of rabbit were extracted immediately after sacrificing the animal; the tissues were frozen to −20°C; the tissues were shaped into cylinder samples in the frozen state; the tissue samples were immersed in liquid nitrogen; and finally, the samples were loaded in a constant strain rate up to a final failure. Tissue samples were taken for histological observation from each stage of the above freezing–loading protocol, including tissue samples which had experienced elastic recoverable deformations only, tissue samples which had experienced permanent (plastic) deformations, and tissue samples which had experienced complete failure.

No significant gross histological damage has been observed in the thawed liver samples due to either processing the tissue in the frozen state, due to slow cooling of the liver tissues down to −20°C or due to rapid cooling of the samples down to −196°C. The region affected by processing the tissue samples in the frozen state had an average thickness of 0.1 to 0.2 mm. No cracks associated with mechanical stress have been observed in the tissue samples which were not loaded by an external load. No histological changes were observed in tissue samples that were loaded within the elastic regime, that is, below the yield strength of the material. Therefore, one may conclude that histological changes due to mechanical stresses are associated with plastic (permanent) deformations. Furthermore, one may conclude that the thermal stresses developed during the cooling stages of the above freez-

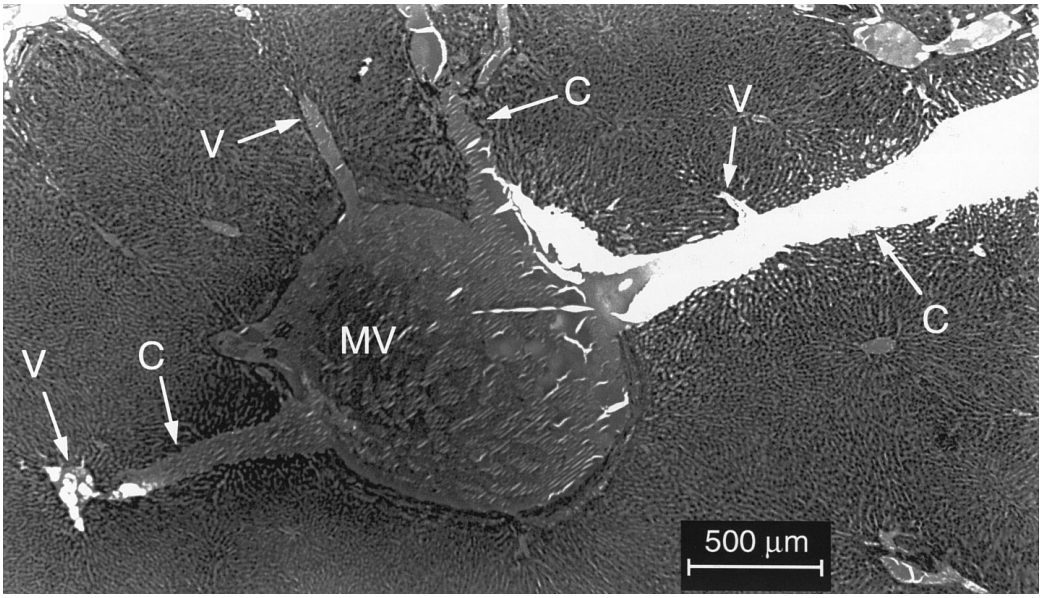

FIG. 10. Crack (C) which has formed in the vicinity of a major blood vessel (MV), which represents a substantial irregularity in the frozen medium. Cracks or damage in materials tend to initiate in regions of inhomogeneity where the stresses tend to be higher. Such irregularities may also arrest propagating crack. Cracks and blood vessels can be easily distinguished in this high magnification view: the crack surfaces consist of fractured cells, while the blood vessels walls are smooth and darker.

ing–loading protocol did not reach the yield strength of the frozen tissue.

Histological observations indicate that linear cracks were developed due to mechanical load beyond the yield strength of the frozen tissue, which appear to have no preferred orientation. These cracks accumulate until final failure of the frozen tissue, when the tissue sample collapses into rubble. One expects that the cracks initiate near irregularities in the frozen medium, which cause stress concentration. On the other hand, the same irregularities in the frozen medium can also arrest crack propagation. Significant sources of such irregularities, in an homogeneous tissue such as the liver, are blood vessels and bile ducts. Indeed, it appears, from the histological observations, that the cracks are associate with such irregularities. Cells along the cracks appeared to have sharp edges without pieces being torn away. Large empty spaces between cells along the cracks indicate a loss of the cells integrity retention of the intracellular solution after the formation of the adjunct crack.

ACKNOWLEDGMENT

This research was supported in part by Allegheny-Singer Research Institute (96-026-2P), Pittsburgh, PA.

REFERENCES

1. Archer, G. P., Kennedy, C. J., and Pegg, D. E. Determination of the volume changes associated with freezing solutions of dimethyl sulphoxide. *Cryo-Lett.* **17,** 3–6 (1996).
2. Fahy, G. M., MacFarlane, D. R., Angell, C. A., and Meryman, H. T. Vitrification as an Approach to Cryopreservation. *Cryobiology* **21,** 407–426 (1984).
3. Fahy, G. M., Saur, J., and Williams, R. J. Physical problems with the vitrification of large biological systems. *Cryobiology* **27,** 492–510 (1990).
4. Fletcher, N. H. ''The Chemical Physics of Ice'' Cambridge Univ. Press, Cambridge, England, 1970.
5. Gao, D. Y., Lin, S., Watson, P. F., and Critser, J. K. Fracture phenomena in an isotonic salt solution during freezing and their elimination using glycerol. *Cryobiology* **32,** 270–284 (1995).

6. Gage, A. A., Guest, K., Montes, M., Garuna, J. A., and Whalen, D. A., Jr. Effect of varying freezing and thawing rates in experimental cryosurgery. *Cryobiology* **22,** 175–182 (1985).
7. Hunt, C. J., Song, Y. C., Bateson, A. J., and Pegg, E. D. Fractures in cryopreserved arteries, *Cryobiology* **31,** 506–515 (1994).
8. Ishiguro, H., and Rubinsky, B. Mechanical interaction between ice crystals and red blood cells during directional solidification, *Cryobiology* **31,** 483–500 (1994).
9. Mazur, P. Kinetics of water loss from cells at subzero temperatures and the likelihood of intracellular freezing. *J. Gen. Phys.* **44,** 347–369 (1963).
10. Mazur, P., Leibo, S., and Chu, E. H. Y. A two-factor hypothesis of freezing injury. *Exp. Cell Res.* **71,** 345–355 (1972).
11. McGrath, J. J. Low temperature injury processes. *In* ''Advances in Bioheat and Mass Transfer'' (R. B. Roemer, Ed.) ASME HTD, Vol. 268, pp. 125–132, 1993.
12. Meryman, H. T. Freezing injury and its prevention in living cells. *Annu. Rev. Biophys. Bioeng.* **3,** 341–363 (1974).
13. Miller, R. H., and Mazur, P. Survival of frozen-thawed human red cells as a function of cooling and warming velocities. *Cryobiology* **13,** 404–414 (1976).
14. Paterson, M. S., ''Experimental Rock Deformation—The Brittle Field.'' Springer-Verlag, Berlin, 1978.
15. Rabin, Y., and Steif, S. P. Analysis of thermal stresses around cryosurgical probe. *Cryobiology* **33,** 276–290 (1996).
16. Rabin, Y., Steif, S. P., Taylor, M. J., Julian, T. B., and Wolmark, N. An experimental study of the mechanical response of frozen biological tissues at cryogenic temperatures. *Cryobiology* **33,** 472–482 (1996).
17. Richerson, D. W. ''Modern Ceramic Engineering,'' 2nd Ed. Dekker, New York, 1992.
18. Rubinsky, B., Cravalho, E. G., and Mikic, B. Thermal stress in frozen organs. *Cryobiology* **17,** 66–73 (1980).
19. Weeks, W., and Assur, A. ''The Mechanical Properties of Sea Ice.'' Cold regions Research & Engineering Laboratory, US Army, Hanover, New Hampshire, 1967.